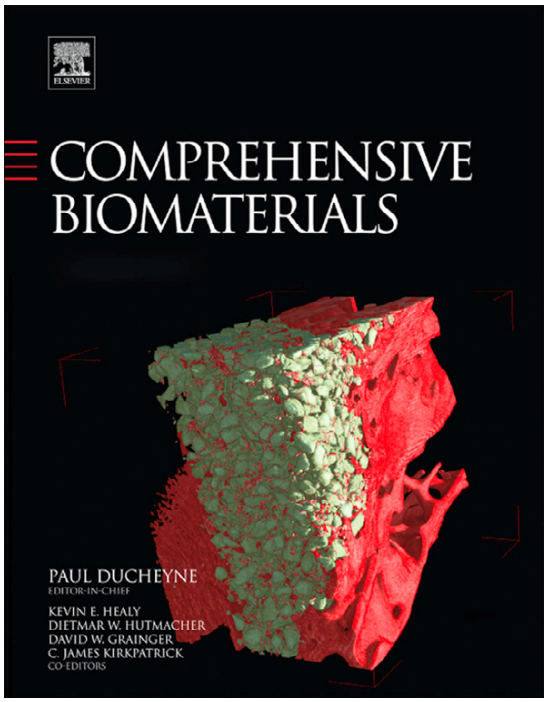

Kohn D.H. (2011) Porous Coatings in Orthopedics. In: P. Ducheyne, K.E. Healy, D.W. Hutmacher, D.W. Grainger, C.J. Kirkpatrick (eds.) Comprehensive Biomaterials, vol. 6, pp. 65-77 Elsevier.

6.605. Porous Coatings in Orthopedics

D H Kohn, University of Michigan, Ann Arbor, MI, USA

Abbreviations

Ac	Acicular
AC	Alternating current
BAA	Beta annealing and aging heat treatment
BCC	Body-centered cubic
COD	Crack opening displacement
CP Ti	Commercially pure titanium
DC	Direct current
DCPD	Dicalcium phosphate dihydrate
EA	Equiaxed
FCI	Fatigue crack initiation
FCC	Face-centered cubic
HA	Hydroxyapatite
HAT	Hydrogen alloying treatment
HCF	High cycle fatigue
HCP	Hexagonal close packed
HIP	Hot isostatic pressing
L	Lamellar
LFCP	Long fatigue crack propagation
MCP	Monocalcium phosphate
MCPH	Monohydrate calcium phosphate
N	Number of fatigue cycles
OCP	Octacalcium phosphate
PEG	Polyethylene glycol
PLGA	Polylactic–glycolic acid copolymer
RNA	Ribonucleic acid
SEM	Scanning electron microscopy
SFCP	Short fatigue crack propagation
STM	Scanning tunneling microscopy
STP	Standard temperature and pressure
TCP	Tricalcium phosphate

6.605.1. Introduction

6.605.1.1. Objectives of Joint Replacement

The clinical objectives of joint replacement are to relieve pain and increase mobility. To meet this objective, material choice and design decisions must provide as physiologic a strain as possible to the bone surrounding the prosthesis so that the integrity and functionality of the bone and implant are maintained over an expected service life of 10–15 years. Materials suited for joint replacements are those that are well-tolerated by the body and can withstand cyclic loading on the order of 10^7 cycles in an aqueous, protein enriched environment.

Total joint replacements are categorized by the mechanism of fixing the implant to the surrounding tissue. In general, implants are either cemented or cementless, referring to whether the implant is stabilized with a grouting agent or by direct contact between tissue and the implant surface. Problems with cemented implants, especially in younger patients, inspired cementless implants in which fixation is dependent upon tissues' ability to bond with the implant and maintain this bond over time.[1–5]

The design of joint replacements is geared toward maximizing interfacial bonding and stress transfer across the implant/tissue interface, within the constraints of using materials that can meet the mechanical demands and be tolerated biologically. Parameters dictating the success of porous-coated joint replacements (Figure 1) include the mechanical properties of the implant, coating, and implant/coating interface[6–10]; mechanisms of tissue attachment to the implant, including

the surface state of the implant and coating, and size, shape, and distribution of surface porosity[11–18]; the mechanical properties of the tissue, including stress and strain magnitude and distribution[19–21]; the elastic properties of the implant, coating and tissue, especially with respect to mediating relative motion and tissue adaptation[22–27]; initial stability and strategies to stimulate tissue ingrowth[28–34]; implant design[35–37]; and the biological response to the implant materials.[38,39]

6.605.1.2. Objectives of Biological Fixation Using Porous Materials

Cementless fixation is achieved by establishing an interference fit between the implant and surrounding tissue. Cementless implants are designed to minimize the time necessary for tissue integration and maximize interfacial stability. Ideally, the implant materials should elicit the formation of normal tissue at the surface and establish a continuous interface capable of supporting service loads over time.[40]

Cementless fixation may be achieved via surface active materials, surface textured materials, or porous-coated materials. Surface active materials lead to fixation through a chemical reaction between tissues and a bioactive implant surface.[41] With surface textured materials, bone grows onto the surface of a grooved or textured implant.[6,42,43] With porous-coated materials, bone grows into the pores of a three-dimensional (3D) porous or porous-coated material.[13,18]

Porous-coated prostheses provide fixation to bone by creating an interdigitation between bone and a porous 3D surface.[12,13,44] Porous-coated systems can lead to a higher bone/implant shear strength than other types of fixation,[12,45] resulting in a better stress transfer from the implant to the surrounding bone, a more uniform stress distribution between the implant and bone, and lower stresses in the implant.[44,46]

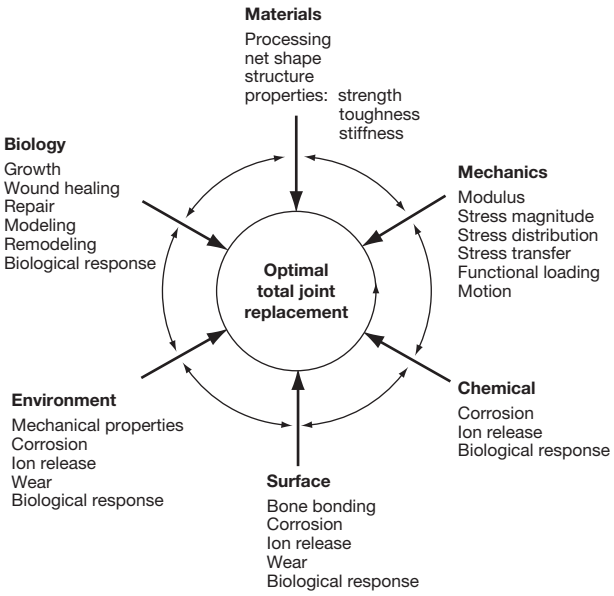

Figure 1 Schematic of interdependent factors affecting the success of porous-coated implants. Reproduced from Kohn, D. H.; Ducheyne, P. In *Medical and Dental Materials*; Williams, D. F., Ed.; VCH, Verlagsgesellschaft, FRG, 1992; pp 29–109, with permission.

6.605.2. Materials Used for Porous Coatings

Porous coatings have been fabricated from polymers – polytetrafluoro-ethylene,[47,48] polysulfone,[43,49] polyethylene,[50] and poly(methylmethacrylate),[51] ceramics – calcium aluminate[52] and alumina,[53,54] and metals – stainless steel,[55] cobalt-based alloys,[18] titanium-based alloys,[13] and tantalum.[56]

6.605.2.1. Metals

Implant materials may corrode and/or wear leading to the generation of particulate debris, which may elicit local and systemic responses. Although metals exhibit high strength and toughness, they are more susceptible to electrochemical degradation than ceramics or polymers. Therefore, a fundamental criterion for choosing a metallic implant material, especially one that will be used as a porous coating with a high surface area, is that the biological response it elicits is minimal. Because of the combined mechanical and environmental demands, metals currently used for porous coatings in orthopedics are limited to three classes: cobalt-based alloys, titanium-based materials, and tantalum. Each of these materials is well-tolerated by the body because of its passive oxide layer.

Porous metal coatings are manufactured from powdered microspheres,[18] fibers,[13] wires,[55] foams,[57] or other porous conglomerates,[58] which are mechanically or chemically bonded onto a dense metallic substrate to produce periodic or inhomogeneous porous surface geometries that vary in porosity and degree to which the porous medium is open or closed (**Figure 2**).

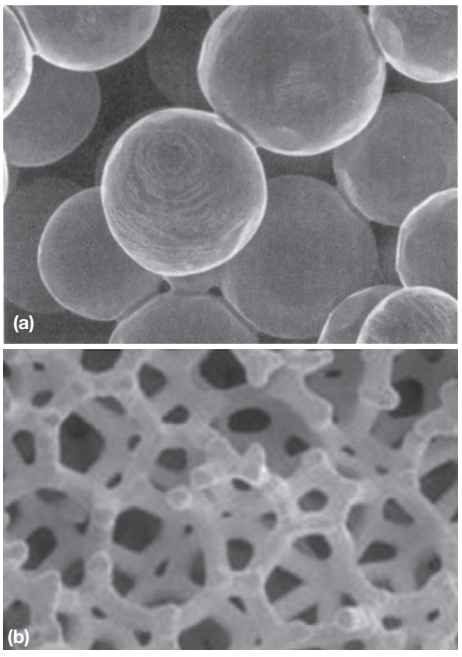

Figure 2 Images of porous metals used in orthopedics. (a) Scanning electron micrograph of porous surface made from titanium powder microspheres approximately 300 μm in diameter. Reproduced from Kohn, D. H.; Ducheyne, P. In *Medical and Dental Materials*; Williams, D. F., Ed.; VCH, Verlagsgesellschaft, FRG, 1992; pp 29–109, with permission. (b) Microstructure of Ta trabecular metal. Reproduced from Levine, B. *Adv. Eng. Mater.* **2008**, *10*, 788–792, with permission.

6.605.2.1.1. Cobalt-based alloys

Three cobalt alloys are used as orthopedic implants: Co–28Cr–6Mo, which is cast (ASTM F75), forged (ASTM F799), or wrought (ASTM F1537); Co–20Cr–15W–10Ni, which is wrought (ASTM F90); and Co–35Ni–20Cr–10Mo, which is wrought (ASTM F562) or forged (ASTM 961) (Table 1). The requirements for powdered coatings conform to those of cast Co–28Cr–6Mo (ASTM F1377).

Co–28Cr–6Mo alloys are cast at 1350–1450 °C and exhibit an inhomogeneous, large-grained, cored microstructure. The dendritic regions are Co-rich and the interdendritic regions are a combination of a Co-rich γ-phase, a Cr-rich $M_{23}C_6$ phase, where M is Co, Cr, or Mo, an M_7C_3 phase, and a Cr and Mo-rich σ-phase.[59] Co–28Cr–6Mo alloys exhibit a eutectic point at 1235 °C.[59] At temperatures above the eutectic, local melting of the solute-rich zones occurs. Cooling to below the eutectic yields a microstructure consisting of grain boundary σ, γ, and $M_{23}C_6$, which embrittle the alloy. Since the interdendritic phases reduce ductility and corrosion resistance, Co–28Cr–6Mo is solution annealed at 1225 °C, resulting in the transformation of σ to $M_{23}C_6$ and partial dissolution of the $M_{23}C_6$ phase.[60]

Wrought Co–Cr has an austenitic microstructure. Forging above 650 °C results in elongated grains, without recrystallization of the austenitic structure, whereas cold-working below 650 °C results in the formation of an ε-phase. Forging results in a smaller grain size and finer distribution of the block carbides than casting.

Co–35Ni–20Cr–10Mo also has a fine-grained austenitic microstructure. This alloy undergoes an allotropic phase transformation, from an HCP to an FCC structure at 650 °C. Similar to Co–28Cr–6Mo, the low-temperature FCC phase is retained upon cooling, with the transformation product existing only within narrow HCP bands. Aging within the two-phase field leads to the formation of a Co_3Mo precipitate in the HCP regions.

Porous-coated Co–Cr–Mo alloys are created by sintering powdered Co–Cr–Mo microspheres, 100–300 μm in diameter onto a Co–Cr–Mo substrate at 1200–1300 °C for 1–3 h. Alternatively, some coatings are formed by plasma-spraying irregular particles onto a substrate. Since sintering temperatures are above the eutectic point,[59] localized melting accelerates particle bonding. However, processing at temperatures in this range results in the formation of eutectic phases and grain boundary carbides, reducing ductility.

6.605.2.1.2. Titanium-based materials

The combination of high strength, resistance to electrochemical degradation, benign biological response, and relatively low modulus make titanium-based materials attractive for load-bearing applications. Commercially, pure titanium does not possess sufficient strength for orthopedic load-bearing applications, but it is used for porous coatings. Several titanium alloys provide sufficient strength and corrosion resistance: Ti–6Al–4V, wrought (ASTM F136) or cast (ASTM F1108); Ti–6Al–7Nb, wrought (ASTM F1295); Ti–13Nb–13Zr, wrought (ASTM F1713); Ti–15Mo, wrought (ASTM F2066) (Table 2). Several new Ti alloys have also been investigated: Ti–5Al–2.5Fe,[61] Ti–12Mo–6Zr–2Fe, and Ti–35Nb–7Zr–5Ta.[62] Of these alloys, Ti–6Al–4V is the most extensively characterized and used. Porous coatings are comprised of commercially pure Ti or Ti–6Al–4V (ASTM F1580).

At room temperature, Ti–6Al–4V is a two-phase α + β alloy. Above the β-transition temperature (975 °C), an allotropic phase transition occurs, transforming the microstructure to a single-phase body-centered cubic (BCC) β-alloy. Heat treating Ti alloys varies the relative amounts of α- and β-phases and morphologies, resulting in a variety of microstructures and

Table 1 Chemical composition (wt%) of cobalt–chromium alloys used in total joint replacement

Element	*Co–28Cr–6Mo*				*Co–20Cr–15W–10Ni*	*Co–35Ni–20Cr–10Mo*
	F75 (cast) + F1377 (powder)	*F799 (forged) + F1537 (wrought)*			*F90 (wrought)*	*F562 (wrought) + F961 (forged)*
		Low carbon	*High carbon*	*Dispersion strengthened*		
Cr	27.0–30.0	26.0–30.0	26.0–30.0	26.0–30.0	19.0–21.0	19.0–21.0
Mo	5.0–7.0	5.0–7.0	5.0–7.0	5.0–7.0		9.0–10.5
Ni	0.5 (max)	1.0 (max)	1.0 (max)	1.0 (max)	9.0–11.0	33.0–37.0
Fe	0.75 (max)	0.75 (max)	0.75 (max)	0.75 (max)	3.0 (max)	1.0 (max)
C	0.35 (max)	0.14 (max)	0.15–0.35	0.14 (max)	0.05–0.15	0.025 (max)
Si	1.0 (max)	1.0 (max)	1.0 (max)	1.0 (max)	0.4 (max)	0.15 (max)
Mn	1.0 (max)	1.0 (max)	1.0 (max)	1.0 (max)	1.0–2.0	0.15 (max)
W	0.2 (max)				14.0–16.0	
P	0.02 (max)				0.04 (max)	0.015 (max)
S	0.01 (max)				0.03 (max)	0.010 (max)
N_2	0.25 (max)	0.25 (max)	0.25 (max)	0.25 (max)		
Al	0.1 (max)			0.30–1.0		
Ti	0.1 (max)					1.0 (max)
B	0.01 (max)					0.015 (max)
La				0.03–0.2		
Co	Balance	Balance	Balance	Balance	Balance	Balance

Table 2 Chemical composition (wt%) of titanium and titanium alloys used in total joint replacement

Element	*c.p. Ti*	*Ti–6Al–4V*			*Ti–6Al–7Nb*	*Ti–13Nb–13Zr*	*Ti–15Mo*
	F1580 (powder)	*F136 (wrought)*	*F1108 (cast)*	*F1580 (powder)*	*F1295 (wrought)*	*F1713 (wrought)*	*F2066 (wrought)*
N_2	0.05 (max)	0.05 (max)	0.05 (max)	0.05 (max)	0.05 (max)	0.05 (max)	0.05 (max)
C	0.08 (max)	0.08 (max)	0.10 (max)	0.08 (max)	0.08 (max)	0.08 (max)	0.10 (max)
H_2	0.05 (max)	0.012 (max)	0.015 (max)	0.015 (max)	0.009 (max)	0.012 (max)	0.015 (max)
Fe	0.50 (max)	0.25 (max)	0.30 (max)	0.30 (max)	0.25 (max)	0.25 (max)	0.10 (max)
O_2	0.40 (max)	0.13 (max)	0.20 (max)	0.20 (max)	0.20 (max)	0.15 (max)	0.20 (max)
Cu				0.10 (max)			
Sn				0.10 (max)			
Y				0.005 (max)			
Ta					0.5 (max)		
Al		5.5–6.5	5.5–6.75	5.5–6.75	5.5–6.5		
V		3.5–4.5	3.5–4.5	3.5–4.5			
Nb					6.5–7.5	12.5–14.0	
Zr						12.5–14.0	
Mo							14.0–16.0
Ti	Balance	Balance	Balance	Balance	Balance	Balance	Balance

range of mechanical properties, depending on whether heat treatments were performed above or below the β-transition temperature and cooling rate.

Thermal treatments below the β-transition temperature produce recrystallized equiaxed microstructures, characterized by small (3–10 μm), rounded α-grains with aspect ratios near unity. This type of microstructure is recommended for Ti–6Al–4V implants (ASTM F136). Thermal treatments above the β-transition temperature lead to a variety of microstructures, depending on cooling rate in the $(\alpha+\beta)$ field. Slow cooling produces a lamellar microstructure, similar to that produced by casting and high-temperature sintering of porous coatings, and characterized by coarse (5–20-μm thick) parallel α-platelets. Lamellar microstructures may be refined via solution treatments above the β-transus and subsequent aging at a temperature high in the $(\alpha+\beta)$ phase field.[7,63,64] Titanium microstructures may also be refined by chemical alloying,[65–68] resulting in microstructures with α-grain sizes <1 μm, aspect ratios near unity and discontinuous grain boundary α, microstructural attributes which increase fatigue strength.

To produce sufficient energy to bond Ti microspheres or particles to a substrate, sintering temperatures in the range of 1200–1400 °C are necessary.[5] At these temperatures, bonding of titanium occurs by solid state diffusion. Temperatures in the 1200–1400 °C range are above the β-transition temperature of most Ti alloys used in medicine, leading to coarse lamellar microstructures. The notch-sensitivity of titanium, along with the lamellar microstructure and surface changes created by high-temperature sintering, lead to a significant reduction in fatigue strength of porous-coated Ti implants versus noncoated implants.

Fiber or wire mesh coatings may be bonded to the substrate using a combination of temperature and pressure. The use of pressure allows for lower sintering temperatures. Therefore, Ti–6Al–4V can be sintered at temperatures below the β-transition temperature,[69] resulting in the retention of an equiaxed microstructure. Other porous coatings, such as ones formed from powdered microspheres, become too dense when subjected to pressure, reducing the porosity below the minimum level necessary for bone ingrowth.

On average, bone only grows into 30% of the total available pore spaces in porous-coated implants and is limited to outer regions of porous coatings.[70] To provide porous surfaces with a higher degree of porosity, without compromising mechanical properties, open cell foams, some mimicking the architecture of trabecular bone, have been developed.[57] Starting with an organic foam shell precursor, metal, typically titanium or tantalum, is coated onto the pore surfaces using vapor deposition and sintered to the bulk implant, resulting in porosities of 60–80%.

6.605.2.1.3. Tantalum

Porous tantalum foams are developed from pyrolysis of an organic precursor into a vitreous carbon skeleton.[57] Subsequently, crystalline tantalum is deposited into the foam via chemical vapor deposition.[56] Modifying the thickness of the Ta layer controls stiffness, strength, and porosity. Nominally, physical properties of Ta foams are in the range of trabecular bone properties: stiffness 3 GPa, compressive strength 60 MPa.[71,72] The larger, more open and regular porosity can lead to bone ingrowth through the full thickness of the coating, filling as much as 80% of the pores and leading to higher fixation strength.[56] Applications of porous Ta include hip and knee arthroplasty, especially revision cases, treatment of osteonecrosis of the femoral head, spinal fusion cages, and use as a structural bone graft substitute.[73,74]

6.605.2.2. Ceramics and Ceramic-Coated Metals

Ceramics were originally used in medicine and dentistry because of their relative biological inertness compared to metals. Over time, emphasis has shifted toward bioactive ceramics, or ceramics that can form a chemical gradient and chemical bond with bone through surface dissolution and ion exchange. In addition to having the ability to bond to bone, ceramics are also used to deliver cells, proteins, and genes.

The most common bioceramic used in orthopedics is hydroxyapatite (HA; $Ca_{10}(PO_4)_6(OH)_2$). The motivation for using synthetic HA as a biomaterial stems from the hypothesis that a biomaterial with a composition similar to the mineral phase in bone will bond to bone. The crystal structure of HA is modified by ionic substitutions, which influence bone bonding. Most synthetic HA implants contain substitutions for the PO_4^{3-} and/or OH^- groups and vary from the ideal stoichiometry and Ca/P ratio of 1.67. For example, oxyhydroxyapatite, tricalcium phosphate, tetracalcium phosphate, and octocalcium phosphate have all been detected in commercially available apatite implants (**Table 3**).[75–78]

Bioactive ceramics exhibit low tensile strength and fracture toughness. Therefore, their use in bulk form is limited to applications in which only compressive loads are applied. Bioactive ceramics may be implanted in anatomic sites subjected to tensile stresses if they are used as a coating on a metal or ceramic implant[29] or strengthened via crystallization or reinforcing with a second phase.[79–82]

Calcium-phosphate coatings have been deposited onto porous metal implants to accelerate bone ingrowth, increase the strength of the prosthesis/bone interface, and shield tissues from metallic corrosion products.[29,70,83] The amount of bone ingrowth, strength of the ceramic/bone interface, degree of improvement in bond strength relative to noncoated metals and Ca-P solubility are variable, suggesting material and processing induced variance in the ceramic and metal, in addition to biological variability.[76,84]

Calcium-phosphate coatings are bonded to metallic implants via several techniques: sintering[75,76,85]; plasma-spraying[77,86]; ion beam and other sputtering techniques[87,88]; electrophoretic deposition[75,76]; sol–gel techniques[89]; pulsed laser deposition[90]; chemical vapor deposition[91]; and solution techniques.[92–95]

Table 3 Calcium-phosphate phases with corresponding Ca/P ratios

Name	*Formula*	*Ca/P ratio*
Hydroxyapatite (HA)	$Ca_{10}(PO_4)_6(OH)_2$	1.67
Fluorapatite	$Ca_{10}(PO_4)_6F_2$	1.67
Chlorapatite	$Ca_{10}(PO_4)_6Cl_2$	1.67
A-type carbonated apatite (unhydroxylated)	$Ca_{10}(PO_4)_6CO_3$	1.67
B-type carbonated hydroxyapatite (dahllite)	$Ca_{10-x}[(PO_4)_{6-2x}(CO_3)_{2x}](OH)_2$	$\geq$1.67
Mixed A and B-type carbonated apatites	$Ca_{10-x}[(PO_4)_{6-2x}(CO_3)_{2x}]CO_3$	$\geq$1.67
HPO_4-containing apatite	$Ca_{10-x}[(PO_4)_{6-x}(HPO_4)_x](OH)_{2-x}$	$\leq$1.67
Monohydrate calcium phosphate (MCPH)	$Ca(H_2PO_4)_2{\cdot}H_2O$	0.50
Monocalcium phosphate (MCP)	$Ca(H_2PO_4)_2$	0.50
Dicalcium phosphate dihydrate (DCPD)	$Ca(HPO_4){\cdot}2H_2O$	1.00
Tricalcium phosphate (TCP)	α- and β-$Ca_3(PO_4)_2$	1.50
Octacalcium phosphate (OCP)	$Ca_8H(PO_4)_6{\cdot}5H_2O$	1.33

Adapted from Segvich, S. J.; Luong, L. N.; Kohn, D. H. In *Biomaterials and Biomedical Engineering*; Ahmed, W., Ali, N., Öchsner, A., Eds.; Trans Tech Publications: Zurich, 2008, with permission.

During plasma-spraying, powder is sprayed onto the metal implant, with plasma temperatures as high as 10 000 °C. The ceramic particles form a loosely bonded coating on impact. Due to the rapid cooling of the particles, the temperature of the metal does not exceed 150 °C and the structure and properties of the bulk metal do not change. However, porosity and phase changes are induced in the ceramic, and mixtures of HA, TCP, and tetracalcium phosphate evolve from stiochiometric HA.[77]

During ion sputtering, an ion beam sputters off atoms from a target to form a thin coating on the porous metal. With electrophoretic deposition, the Ca-P coating is precipitated out of suspension onto the metal implant. Electrophoretic deposition is more conducive to coating the internal surfaces of a porous metal. Both sintering and electrophoretic deposition of apatite on titanium result in a phosphate-rich interfacial layer.[75] The interior of the coating is phosphate-depleted, resulting in a higher Ca/P ratio, the formation of tetracalcium phosphate and increased solubility.

An apatite layer can also be formed on an implant surface *in vitro* under STP conditions.[92,93,95–99] The use of biomineralization strategies to form 'bone-like mineral' *in vitro* is based on the concept that bioactive ceramics can bond to bone through a layer of bone-like apatite, which forms on some ceramic surfaces *in vivo* and is characterized as a carbonate-containing apatite with nanoscale crystallites.[100–103] It is therefore hypothesized that a requirement for a biomaterial to bond to bone is the formation of a biologically active bone-like apatite layer.[100–103]

The deposition of apatite onto an implant surface from solution is guided by the pH and ionic concentration of the microenvironment. Conditions conducive to heterogeneous nucleation will support epitaxial growth of mineral. To drive heterogeneous precipitation of mineral nuclei, the net energy between a nucleated precursor and the substrate must be less than the net energy of the nucleated precursor within the ionic solution.[93] The surface energy of an implant may be altered and functional groups that can chelate calcium ions may be created by grafting, self-assembled monolayers, irradiation, alkaline treatment, or hydrolysis.[95,97,99,104,105] Biomimetic strategies have been used to coat metals to accelerate osseointegration,[92,96,98,104,106] as well as glasses, ceramics, and polymers.[95,97,99,105,107,108]

The self-assembly of apatite within the pores of a porous or porous-coated implant enhances cell adhesion, proliferation, and osteogenic differentiation, as well as modulates cytoskeletal organization and cell motility *in vitro*.[109] When progenitor cells are transplanted on these materials, a larger and more spatially uniform volume of bone is regenerated.[110] An additional benefit of the biomimetic processing conditions is that growth factors can be incorporated into the coating without denaturing, enabling a dual conductive/inductive approach.[111–113]

Regardless of the technique used to coat an implant with bioactive ceramic, long-term stabilization and fixation strength frequently do not depend on the ceramic coating. The primary benefit of ceramic-coated porous metals is to accelerate the achievement of a steady-state interfacial strength. In addition to characterizing the ceramic/bone interface under functional loading, the mechanical integrity of the metal/ceramic interface must also be considered as a design parameter.

Different structures and compositions of Ca-P coatings result from different processing techniques. Ion exchange reactions at the interface between a ceramic surface and biological environment depend on a comprehensive set of physical/chemical properties, including particle size and shape, pore size, shape and distribution, phases present, crystallinity, coating thickness, hardness, stiffness, roughness, and surface area.[114] Differences in ceramic chemistry and structure lead to differences in biological response both *in vitro* (e.g., cell attachment and proliferation, protein synthesis, RNA transcription)[109,115,116] and *in vivo* (e.g., cell differentiation, amount and rate of bone formation, intensity, or duration of inflammatory response).[117–119] The collective data from numerous animal and human studies are that calcium-phosphate coatings with Ca/P ratios in the range 1.5–1.67, tricalcium phosphate and HA, respectively, result in the most beneficial tissue response.[114]

6.605.2.3. Polymers

Because of stress shielding of bone with stiff metallic implants, it is hypothesized that an isoelastic femoral stem or coating, which has a modulus similar to that of bone, will result in a more uniform stress distribution and better stress transfer across the implant/bone interface, reducing mechanically mediated bone resorption. Since most polymers are not mechanically suitable to be used as bulk load-bearing implants porous polymers, including polytetrafluoro-ethylene,[47,48] polysulfone,[43,49] and polyethylene,[50] have been used as coatings.

Coating metal implants with polymers could circumvent problems arising with porous metal coatings, including reduction in fatigue strength, stress shielding, and release of dissolution products. For example, polymer coatings have a lower modulus, are sintered to Ti–6Al–4V at temperatures below the β-transformation, and decrease the surface area of metal exposed to body fluids.[49] These advantages, however, are outweighed by the inability of the metal–polymer interface to withstand the stresses resulting from functional loading.

Although polymer coatings are used less extensively than metal or ceramic coatings, bone will grow into many polymers that are sufficiently inert and have a suitable porosity. The extent and time course of ingrowth depends on the location of implantation and mode of loading, but, at least from qualitative observations, the integrity of the polymer/bone interface can be as mechanically stable as a metal/bone interface. With the interest in degradable materials for tissue regeneration, porous polymers have experienced a renewed interest.

6.605.3. Properties of Porous-Coated Implants

To achieve bone ingrowth into the surface of an implant, high surface area coatings are used. The surface area of porous-coated implants is five to ten times greater than the surface area of noncoated, nontextured implants. Porous coatings have the potential to provide advantages of biological fixation, increased bone/implant shear strength, better stress transfer from the implant to the surrounding bone, and a more uniform stress distribution. However, the increased surface area does lead to potential, mechanical, and electrochemical disadvantages and design of porous-coated implants requires an understanding of the mechanical and electrochemical consequences of higher surface area materials. Reductions in fatigue and degradation resistance have been implicated in the failure of porous-coated implants.[120–122]

6.605.3.1. Mechanical Properties

Due to the long service life requirements of total joint replacements, the most critical mechanical property is high cycle fatigue strength. For many materials, 90% of the fatigue life is spent initiating a fatigue crack.[123] Thus, microstructural and compositional parameters inhibiting crack nucleation produce good high cycle fatigue strength. However, for materials with voids and geometric irregularities, especially notch-sensitive materials such as titanium, resistance to crack propagation is also a critical design parameter. Because of the microstructural and geometric changes brought about by the deposition of a porous coating onto an implant surface, the high cycle fatigue strength of porous metal implants is approximately 75% lower than the fatigue strength of uncoated total joint replacements[7,8,10,124,125] (**Table 4**).

The high ultimate and fatigue strengths make Co–Cr–Mo alloys suitable for joint reconstruction. However, the fatigue strength of porous-coated Co–Cr–Mo is only 180–250 MPa.[5,60,125] The high-temperature (1200–1300 °C) sintering treatment required to bond the coating to the substrate results in a microstructure similar to the microstructure of cast Co–Cr–Mo, which exhibits porosity and eutectic phases. Noncoated implants subject to the same sintering treatment have similar low fatigue strengths.[5,125] The lower fatigue strength of porous-coated Co–Cr–Mo implants can therefore be attributed to sintering, and postsintering treatments sufficient to refine cast microstructures are also applicable to porous-coated Co–Cr–Mo implants.[60,125]

The fatigue strength of Co–Cr–Mo alloys is controlled by the ability of the solute atoms C, Cr, and Mo to inhibit dislocation motion.[60] Solution annealing increases strength and ductility due to a reinforcing effect of the transformed carbides. However, prolonged annealing, such as during sintering treatments, results in more complete carbide dissolution and a decrease in fatigue strength.[60] Hot isostatic pressing (HIP-ing) increases the fatigue strength by reducing porosity and eliminating grain boundary carbides.[125]

The mechanical properties of $(\alpha+\beta)$ titanium alloys are dictated by the amount, size, shape, and morphology of the α-phase and the density of α/β interfaces.[114,126–128] Microstructures with a small α-grain size, a well dispersed β-phase, and a small α/β interface area, such as equiaxed and H_2-alloyed microstructures, resist fatigue crack initiation best and have the highest fatigue strengths (500–700 MPa),[8,67,127–129] because a small α-grain size decreases the slip length. Lamellar microstructures, which have a larger α/β surface area and more oriented colonies, have lower fatigue strengths (300–500 MPa), because slip is more easily transmitted from one plate to another. Hydrogen-alloying treatments break up the continuous grain boundary α and colony structure and produce a homogeneous microstructure consisting of refined α-grains in a matrix of discontinuous β, resulting in increased fatigue strength.[67]

Table 4 Fatigue strengths of porous-coated metals

Material	*Treatment*	*Fatigue strength (MPa)*	*Testing parameters*	*Authors*
Co–Cr–Mo	As cast	267	Reverse bending ($R = -1$); 167 Hz; $N = 2 \times 10^7$	Georgette and Davidson[125]
	Sintered + HT[a]	177		
	Sintered + HIP + HT	255		
	Porous-coated, sintered + HT	193		
	Porous-coated, sintered + HIP + HT	234		
Ti–6Al–4V	Wrought	625	Reverse bending ($R = -1$); 50 Hz; $N = 10^7$	Yue *et al.*[10]
	β-sintered	500		
	Porous-coated, β-sintered	200		
	Wrought	617	Reverse bending ($R = -1$); 167 Hz; $N = 5 \times 10^7$	Cook *et al.*[124]
	β-sintered	377		
	Porous-coated, β-sintered	138		
	Wrought	668	Reverse bending ($R = -1$); 167 Hz; $N = 5 \times 10^7$	Cook *et al.*[7]
	β-sintered	394		
	β-sintered + BAA-1[b]	488		
	β-sintered + BAA-2[b]	494		
	Porous-coated, β-sintered	140		
	Porous-coated, β-sintered + BAA-1	161		
	Porous-coated, β-sintered + BAA-2	162		
	Wrought	590	Reverse bending ($R = -1$); 100 Hz; $N = 10^7$	Kohn and Ducheyne[8]
	β-sintered	497		
	β-sintered + HAT-1[c]	669		
	β-sintered + HAT-3[c]	643		
	β-sintered + BAA-3[b]	538		
	Porous-coated, β-sintered	218		
	Porous-coated, β-sintered + HAT-3	177		
	Porous-coated, β-sintered + BAA-3	233		

Modified from Kohn, D. H.; Ducheyne, P. In *Medical and Dental Materials*; Williams, D. F., Ed.; VCH: Verlagsgesellschaft, FRG, 1992; pp 29–109, with permission.

[a]Proprietary postsintering heat treatment.

[b]BAA = postsintering beta annealing and aging treatment: BAA-1 = 1250 °C, 2 h, slow cool; BAA-2 = 1250 °C, 2 h, slow cool/Ar cool/(α + β) anneal, 4 h, Ar cool BAA-3 = 1030 °C, 20 min, Ar quench/540 °C, 4 h, Ar quench.

[c]HAT = postsintering hydrogen-alloying treatments: HAT-1 = 850 °C, 0.5 h in H_2/650 °C, 16 h in vacuum; HAT-3 = 850 °C, 0.5 h in H_2/590 °C, 4 h in Ar/775 °C, 4 h in vacuum.

Since the fatigue life of porous-coated titanium alloys is governed by both the initiation and propagation of fatigue damage, the design of porous-coated implants must also account for mechanisms of fatigue crack propagation, which differ from those governing fatigue crack initiation. Microstructures with large grains and α/β interfacial areas have lower fatigue crack propagation rates and higher threshold stress intensities than fine-grained microstructures.

The reduced fatigue strength of porous-coated Ti is due to a combination of three factors: stress concentrations at the porous coating/substrate interface and within the porous coating: local stresses can be as high as 6X the applied stress[130]; changes in microstructure due to high-temperature sintering: resulting lamellar microstructures have a fatigue strength 20–40% lower than the fatigue strength of wrought, equiaxed Ti–6Al–4V[8,10,67,124,131]; and surface contamination from sintering.[10] Of these three factors, stress concentrations are the most critical.

As the stress concentration in a porous coating increases, the controlling stage of fatigue changes from crack initiation to short crack propagation to long crack propagation (**Figure 3**). As the governing stage of fatigue changes, the microstructure which maximizes the resistance to damage accumulation during that particular stage also changes. At low stress concentrations, crack initiation is the governing stage of fatigue and microstructures with small grains have the highest fatigue strength. At high stress concentrations, fatigue is governed by long crack propagation and coarse microstructures have the highest fatigue strength. At intermediate stress concentrations, such as the stress concentrations at sinternecks, there is no effect of microstructure, since fatigue life is equally dependent on crack initiation and crack propagation. Current porous coating designs lie in the crack propagation region of **Figure 3**. Reducing the stress concentrations at the porous coating/substrate interface will enable postsintering treatments to increase the fatigue strength of porous-coated titanium implants.

6.605.3.2. Electrochemical Properties

Corrosion and wear of implants are undesirable because of potential biological reactions to the degradation products

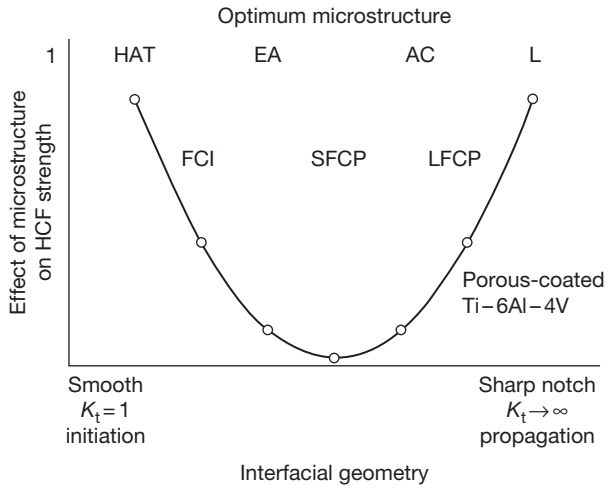

Figure 3 Schematic of Ti–6Al–4V high cycle fatigue (HCF) strength and governing stages of fatigue (FCI, fatigue crack initiation; SFCP, short crack propagation; LFCP, long fatigue crack propagation) as functions of microstructure (HAT, hydrogen alloy treated; EA, equiaxed; AC, acicular; L, lamellar) and interfacial geometry. Reproduced from Kohn, D. H.; Ducheyne, P. In *Medical and Dental Materials*; Williams, D. F., Ed.; VCH: Verlagsgesellschaft, FRG, 1992; pp 29–109, with permission.

and potential loss of implant structural integrity. For these reasons, metals used in implantology are in their passive state under typical physiological conditions and, theoretically, breakdown of passivity and transport of metal ions and electrons across the metal oxide should not occur.

Cobalt–chromium alloys are corrosion resistant because of their passive chromium oxide layer. Alloying with Mo further enhances corrosion resistance.[60] The inhomogeneous microstructure of cast Co–Cr–Mo makes it more susceptible to corrosion than the forged alloy,[132] due to the presence of Cr-depleted dendritic regions acting as the more anodic sites in a galvanic reaction. Wrought Co–Cr–Mo has a lower carbon content than cast Co–Cr–Mo and, as a result, a lower corrosion resistance.[132] However, the rest potentials of Co–Cr alloys are below the breakdown potential, and the breakdown potential exceeds the potential of the oxygen reduction reaction.[133] In addition to the increased surface area of porous-coated Co–Cr alloys, sintering causes microstructural changes that also decrease corrosion resistance behavior. For example, in sintered Co–Cr, corrosion preferentially occurs at grain boundaries and regions adjacent to carbides.[134] Both c.p. Ti and Ti–6Al–4V possess excellent corrosion resistance for a full range of oxide states and pH levels. The low dissolution rate and near chemical inertness of titanium dissolution products allow bone to osseointegrate with titanium.[133]

Even in their passive condition, however, metals are not inert, and passive dissolution occurs from the surfaces of metals used in orthopedics. Corrosion of a metal (oxidation/reduction reactions and the rate of these reactions) is dictated by thermodynamic driving forces and kinetics. Corrosion may be an independent process or act in concert with wear. Even if uncoupled, neither corrosion nor wear operates via a single or spatially uniform mechanism. For example, corrosion may occur globally over a large region of an implant surface or locally at sites of different surface or solution concentration. Under functional loading, which can involve relative motion, fretting or wear between components, corrosion can be mechanically assisted. Fretting corrosion, corrosion fatigue and stress corrosion cracking can accelerate the release of metal ions or particulates. Dynamic metal-on-metal contact can occur in metal–metal wear couples and in tapered connections in modular prostheses and these junctions are especially prone to corrosion, with elevated amounts of corrosion products detected in surrounding tissues.[135–137] If wear particles are generated, then there also exists the potential for these higher surface area particles to undergo dissolution.

Although the biological consequences are unknown, increased concentrations of metal ions occur locally and systemically in patients with metal implants, especially loose implants.[39,138–141] While discolored tissues adjacent to titanium implants are due to metal debris, the elemental ratios in the tissue are similar to those in the bulk alloy, suggesting that the debris represent wear particles rather than corrosion products.[142] Although wear debris present a large surface area for corrosion, it is the presence of wear debris that is the major contributor to systemic increases in titanium.[140] Corrosion products are more prevalent in tissues adjacent to Co–Cr implants, although these products are also associated with modular implants or loosening.[39] During wear accelerated corrosion, Co–Cr alloys can release large amounts of dissolution product during repassivation, due to solution supersaturation at the metal surface. Titanium, on the other hand, repassivates almost instantaneously through surface controlled oxidation kinetics. Titanium ion release that does occur is a result of the chemical dissolution of titanium oxide.

The increased surface area of porous-coated implants increases the potential for passive dissolution or mechanically-assisted degradation. Metal oxide dissolution in porous-coated implants creates several questions that are important to investigate: What material is released? How much is released? What reactions are release products involved in? What percent of the release products is excreted versus retained? If retained, where do these products accumulate? What biological responses result from the retained fraction?[39,143–145]

6.605.4. Design and Characterization of Porous Materials

The complex 3D surface geometry and micromechanical environment within porous materials make the design and characterization of porous-coated implants challenging. The interfaces between the porous coating and implant and porous coating and tissue (hard and soft) also need to be well characterized as part of an effective design approach. Many of the design principles for porous-coated implants translate into the design of porous scaffolds for tissue engineering. The success of both technologies depends on the ability of the microenvironment to help organize cell function in 3D porous media and allow functional tissue to grow and adapt. Understanding the interaction between porous biomaterials and tissue at different dimensional scales is therefore important, and a variety of experimental and analytical approaches are available to characterize this complex microenvironment.

Porous coatings are formed from bonded microspheres, fibers, plasma-sprayed particles, or foams, and can be either open or closed systems of ordered or random architecture. Quantifying architectural parameters and developing structure–property relations is critical, especially considering competing design objectives of maximizing porosity for transport, cellular invasion, and bone ingrowth, but also maximizing strength.

Stereology is well established in metallurgy and stereological principles were adapted for analysis of trabecular bone and other porous and granular media.[146,147] Briefly, test lines oriented at an angle θ are superposed onto planar sections of a porous coating consisting of domains that are defined as either material or void space. The mean intercept length is the average distance between two material/void interfaces measured along a line. When mean intercept length is plotted against direction, the data fit the equation of an ellipse in 2D and an ellipsoid in 3D. From 2D measures of the ratio of material voxels to total voxels and the number of intersections a test line makes relative to its total length, architectural parameters, such as volume fraction, surface-to-volume ratio, thickness, density, and separation can be calculated. The ratios of mean intercept length in orthogonal directions can provide an estimate of the degree of anisotropy. Connectivity of a porous structure and determination of whether a structure is open (connected pores) or closed cell (pores not connected) can be quantified via the determination of an Euler number.

Characterizing the mechanical properties of porous materials is more complicated than for dense, spatially homogeneous materials. Three levels of dimensional scale should be considered: structural properties or properties of the whole domain of material and voids; material properties or properties of individual microspheres, fibers, or struts of trabecular metal; and nanoscale properties or properties on the same dimensional scale as features of the material that interact with cells.

Characterizing the stiffness of porous coatings is important because local stiffness controls cell spreading, cytoskeletal mechanics, and cell differentiation,[148] ultimately affecting bone ingrowth. The stiffness of a porous coating also controls stress transfer, bone adaptation, and stability of the porous coating/tissue interface.[149,150] Gradients in stiffness between porous coatings and the underlying dense implant also affect porous coating/substrate bonding. At the structural-level, porous coatings may be anisotropic, which necessitates testing in multiple directions. Structural-level stiffness–strength relations follow a power law relationship with structural density and, for idealized models of cellular solids, closed form relations for the stiffness of open and closed cell structures exist.[151]

Anisotropic elastic constants of a porous coating/tissue interfacial zone can be predicted via a number of analytical techniques that provide values bounded by load and displacement boundary conditions.[25] The amount and distribution of bone ingrowth into a porous coating and subsequent bone adaptation depend on local strains,[152,153] which are dependent on material and tissue architecture within the implant/tissue interfacial zone.[150,154] Coating design, loading history, and relative motion also affect the amount of bone ingrowth.[27,154,155] Developing relations between local strain magnitude and amount and distribution of ingrown bone is challenging. Most studies focus on bone adaptation to implants on a global level, not accounting for porous coating architecture. However, local tissue distribution surrounding individual microspheres within a whole implant interface is poorly correlated with global mechanical fields. Global models by themselves, unless highly refined and computationally intensive, model the porous coating/tissue interface as a homogeneous bonded interface, and omit local details. Local models of isolated regions of a porous coating are valuable for predicting local stresses and strains, but are typically not linked to an analysis of the whole implant. Scaling local strains to actual tissue strains in relation to physiological loading is needed to establish the relationship between local interface tissue strains and amount of bone ingrowth.

Local models idealize porous coatings into regular, periodic microstructures consisting of idealized shaped unit cells and, in hierarchical analyses, are coupled with global continuum models.[150] Coupled global/local modeling shows that with increased depth of bone ingrowth, stress concentrations in both metal and tissue are reduced, reducing potential mechanical failure at the porous coating/tissue interface.[150,156] Moreover, strain fields around individual microspheres are inhomogeneous and peak strains in the interfacial zone are more than triple the strains predicted by global analyses, demonstrating the need for local analyses.

Because of the stress intensification in porous metals, crack initiation life is not a valid predictor of fatigue life. Therefore, a technique of detecting fatigue crack initiation and monitoring fatigue crack propagation is important for characterizing the mechanical response of porous coatings. In implementing a technique of monitoring fatigue damage in porous materials, several material characteristics must be considered: the complex surface geometry, the potential for damage to occur simultaneously at multiple, unknown sites, and the possibility of irregular crack contours.[157]

A technique of monitoring the structural integrity of a porous material should fulfill the following criteria[157]: (1) detect damage at any location at any time; (2) detect damage at multiple sites that are unknown *a priori*; (3) measure the dimensions of damage; (4) be sensitive, accurate, free of artifact, easily calibrated and implemented; (5) monitor the material continuously during loading; (6) monitor in real-time; (7) be nondestructive; and (8) be applicable to all materials and in all environments. Nondestructive techniques of detecting material flaws and measuring damage may be defined with respect to the physical parameter(s) of the material that the defects alter, and include techniques that measure alterations in mechanical, electrical, magnetic, thermal, acoustic, chemical and optical properties, and particle and wave parameters (**Table 5**).

In summary, a combination of experimental and analytical techniques introduced into biomaterials has yielded insights into the behavior of porous coatings as structural materials and as components of a biomaterial/tissue composite that are critical to the clinical success of porous-coated prostheses.

6.605.5. Porous Coatings in Tissue Engineering

Many of the strategies used to design porous-coated implants can be transferred to the design of porous scaffolds used in

Table 5 Summary of techniques to monitor material damage

Technique	*Advantages*[a]	*Disadvantages*[a]	*Minimum detectable damage zone (μm)*
Acoustic emission	1, 2, 4–8	3, 4	10
Barkhausen noise	1, 2, 5–7	3, 4, 8	–
Compliance/ COD	3, 5–8	1, 2, 4	25
Computed tomography	1–3, 7, 8	4–6	50
Eddy currents	1, 2, 7	3–6, 8	220
Exoelectrons	1, 2, 5–7	3, 4, 8	–
Holography	1, 2, 5–8	3, 4	–
Laser telemetry	3–8	1, 2	0.13
Metallography	2–4, 8	1, 5–7	O(μm)[b]
Microwaves	5–8	1–4	2500
Moire patterns	1, 2, 5–8	3, 4	10
Potential drop – DC	1, 3–7	2, 8	3
Potential drop – AC	1, 3–7	2, 8	10
Radiography	1–4, 6, 7	5, 8	25
SEM	2–4, 8	1, 5–7	0.01
STM	3,8	1, 2, 4–7	O(Å)[b]
Ultrasound	1, 2, 6–8	3–5	2100

Modified from Kohn, D. H. *Crit. Rev. Biomed. Eng.* **1995**, *22*, 221–306, with permission.
[a]Numbers refer to attributes (1)–(8) of damage monitoring techniques listed at Section 4. Numbers listed under advantages mean the technique can meet those requirements, while listings under disadvantages mean those particular requirements cannot be met.
[b]O = on the order of.

tissue engineering for controlling tissue growth. An ideal tissue substitute would satisfy the following design requirements, many of which are design requirements for porous-coated implants[94,158]: biocompatibility; osteoconductivity – it should provide an appropriate environment for attachment, proliferation, and function of osteoblasts or their progenitors, leading to the secretion of new bone; osteoinductivity – it should have the ability to incorporate factors that direct bone growth; sufficient porosity to allow transport and ingrowth of vascular tissue; mechanical integrity to support functional loads; controlled degradation into nontoxic species that are metabolized or excreted; and ability to be easily processed into irregular 3D shapes.

Bone regeneration can be achieved by culturing cells capable of expressing the osteoblast phenotype onto porous synthetic or natural materials that mimic structural and/or functional aspects of natural extracellular matrices. Materials that satisfy at least some of the design requirements for a bone substitute and support bone regeneration include titanium,[34,159] PLGA,[160] collagen,[161] polyphosphazenes,[162] polyurethanes,[163] polycaprolactone,[164] PEG,[165] poly-(propylene fumarate),[166] starch-based materials,[167] alginate,[168] silk,[169] bioactive glasses and glass ceramics,[115,116] HA, TCP, and coral,[119,161,170,171] HA/ and HA/TCP/collagen,[161] and polymer/apatite composites.[97,172–174] Analogous to the findings that the architecture and composition of a porous-coated total joint replacement control tissue ingrowth,[27,154] alterations in scaffold composition and structure can alter *in vitro* outcomes, including osteoblast or progenitor cell attachment and proliferation, collagen and noncollagenous protein synthesis and RNA transcription,[109,116,174–177] as well as *in vivo* outcomes, including progenitor cell differentiation to an osteoblast lineage, amount and rate of bone formation.[117,119,178]

In addition to their osteoconductive nature, porous and porous-coated biomaterials can be combined with inductive factors, to control cell proliferation, differentiation, and bone formation.[113,179,180] Osteoinductive properties can be integrated into a biomaterial by immobilizing proteins or peptides to the material surface via adsorption, cross-linking, covalent binding, or physical entrapment. Each of these immobilization techniques results in different loading efficiencies and different levels of protein retention, as well as influences the release profile of the molecule. Growth factors can be adsorbed to or dispersed over the surfaces of metal, ceramic, and polymer biomaterials, allowing these nonbiologically communicative materials to serve as delivery systems for molecules that can communicate with surrounding cells.[181,182] Although release kinetics are dependent on the material and protein, the general release profile of a surface adsorbed molecule is rapid release, followed by a slower release based on the chemical and/or physical attraction between the material and protein.[183,184] In some cases, a more sustained release or a pulsatile release is required for a growth factor to be effective. Controlled release of a growth factor can be achieved by incorporating the factor into the bulk of a polymer during polymerization and designing a release profile based on protein diffusion and/or material degradation.[185,186] Other means of incorporating proteins into the bulk of a material include using layer-by-layer assembly and adsorbing the protein into each layer deposited,[187] binding pellets together using a gel, with a growth factor adsorbed to the surface of the pellets,[188] using sol–gel techniques to create slow release protein carrier coatings,[189,190] and coprecipitating inorganic/organic coatings onto implants.[111,191]

In order to integrate drug delivery capabilities with other design variables for a porous-coated implant, methodologies that are amenable to encapsulating a drug to the surface of a material that can withstand mechanical loads would have the most impact. Growth factors and antibiotics have been incorporated onto titanium alloy implants by coprecipitating the proteins with calcium phosphate.[179,192] An important advantage to this approach is the ability to produce calcium-phosphate coatings at a physiological temperature, minimizing conditions that would change the biological activity of the factors. The mineral/protein coating can be as thick as 50 μm.[191] Biomolecules can be incorporated at different stages of calcium-phosphate nucleation and growth,[111,193] enabling spatial localization of the molecule through the apatite thickness and increasing protein loading. Coprecipitation therefore results in a more controlled release of biomolecules in comparison to adsorption, because the negatively charged protein has an affinity for the apatite matrix, rather than just a superficial association.[111,191] Techniques used to incorporate growth factors into bone-like mineral can also be used to incorporate genes.[112,194]

6.605.6. Summary and Future Directions

Over the past 40 years, porous-coated implants have been utilized clinically as an alternative to cemented implants, especially in younger and more active patients. In addition to total joint replacements, porous-coated implants are used for segmental defects and as spinal implants. Many of the design objectives learned over the last four decades may also be translated to tissue engineering. Conversely, tissue engineering strategies may come to fruition first when used to augment the function of an implant, rather than regenerate a tissue *de novo*.

The use of porous and porous-coated biomaterials is expected to expand and, although clinically successful, modifications to current technologies could increase the service life and expand the pool of patients with indications for use. There are several areas in which new materials, new designs, and new strategies of creating and maintaining tissue ingrowth could be achieved. New coating materials that have a combination of fatigue resistance and elastic match with bone, yet have sufficient porosity to facilitate transport and are biologically tolerable are needed. A second approach to improve mechanical integrity and cooptimize mechanical and transport properties to modify coating architecture. Architectural modifications include design of functionally graded materials, creation of open cell coatings, and development of optimization algorithms to design coatings in which material is distributed to meet dual objective functions of maximizing strength and maximizing permeability. Design and manufacturing of periodic, open microstructures can be achieved by solid free form fabrication methods, such as 3D fiber deposition, selective laser melting, 3D printing.[195–197]

Strategies to increase the magnitude and rate of bone ingrowth using material chemistry and biological approaches also parallel many strategies used in tissue engineering. In fact, advances in tissue engineering are likely to first arise in conjunction with established implantology approaches and materials. Use of nanomaterials, attachment of biological factors, and integration of drug delivery with implantology may each help enhance bone growth. A variety of cell functions, such as adhesion and intracellular signaling, are sensitive to surface features on the order of nanometers.[198] Creation of nanosized grains or nanoscale topologies on a microscale coating could therefore provide a porous-coated implant with the physical scale necessary to better influence biological function.

Attachment and delivery of proteins from implants is also being pursued.[189,190] Proteins, however, are subject to isolation and degradation. Proteins can also change conformation because they possess sections with varying hydrophobicities. Peptides can mimic the function of a protein while being smaller, cheaper, and less susceptible to degradation. Peptides have the potential for controlling initial biological activity, because they can contain specific target amino acid sequences and can permit control of hydrophilic properties through sequence design. Peptide sequences have been designed to mimic sections of ECM proteins,[199] and material-specific peptides have been discovered.[200]

Modifying surface chemistry and integration of biological molecules with materials to control cell function are important design modifications. By themselves, however, they are not sufficient for clinical function. A key to translating advances in nanotechnology, materials chemistry, and biomolecular surface engineering into the design of a clinically relevant implant is to integrate the nanoscale features needed to control cell function with a larger 3D implant that has the dimensions and bulk properties required to fulfill a desired clinical application.

References

1. Ducheyne, P. In *Functional Behavior of Orthopaedic Biomaterials*; Ducheyne, P., Hastings, G. W., Eds.; Applications; CRC Press: Boca Raton, FL, 1984; Vol. II, pp 163–169.
2. Haddad, R. J.; Cook, S. D.; Thomas, K. A. *J. Bone Joint Surg. Am.* **1987**, *69*, 1459–1466.
3. Hulbert, S. F.; Young, F. A.; Mathews, R. S.; Klawitter, J. J.; Talbert, C. D.; Stelling, F. H. *J. Biomed. Mater. Res.* **1970**, *4*, 433–456.
4. Lemons, J. E. *ASTM STP 953, Quantitative Characterization and Performance of Porous Implants for Hard Tissue Applications*; ASTM: West Conshohocken, PA, 1987.
5. Pilliar, R. M. *Clin. Orthop.* **1983**, *176*, 42–51.
6. Bourassa, P. L.; Yue, S.; Bobyn, J. D. *J. Biomed. Mater. Res.* **1997**, *37*, 291–300.
7. Cook, S. D.; Thongpreda, N.; Anderson, R. C.; Haddad, R. J., Jr. *J. Biomed. Mater. Res.* **1988**, *22*, 287–302.
8. Kohn, D. H.; Ducheyne, P. *J. Biomed. Mater. Res.* **1990**, *24*, 1483–1501.
9. Kohn, D. H.; Ducheyne, P.; Awerbuch, J. *J. Biomed. Mater. Res.* **1992**, *26*, 19–38.
10. Yue, S.; Pilliar, R. M.; Weatherly, G. C. *J. Biomed. Mater. Res.* **1984**, *18*, 1043–1058.
11. Albrektsson, T.; Branemark, P. I.; Hansson, H. A.; *et al. Ann. Biomed. Eng.* **1983**, *11*, 1–27.
12. Bobyn, J. D.; Pilliar, R. M.; Cameron, H. U.; Weatherly, G. C. *Clin. Orthop.* **1980**, *150*, 263–270.
13. Galante, J.; Rostoker, W.; Lueck, R.; Ray, R. D. *J. Bone Joint Surg.* **1971**, *53A*, 101–114.
14. Hacking, S. A.; Harvey, E. J.; Tanzer, M.; Krygier, J. J.; Bobyn, J. D. *J. Bone Joint Surg. Br.* **2003**, *85*, 1182–1189.
15. Healy, K. E.; Ducheyne, P. *Biomaterials* **1992**, *13*, 553–561.
16. Shannon, F. J.; Cottrell, J. M.; Deng, X. H.; *et al. J. Biomed. Mater. Res.* **2008**, *86A*, 857–864.
17. Taché, A.; Gan, L.; Deporter, D.; Pilliar, R. M. *Int. J. Oral Maxillofac. Implants* **2004**, *19*, 19–29.
18. Welsh, R. P.; Pilliar, R. M.; Macnab, I. *J. Bone Joint Surg.* **1971**, *53A*, 963–977.
19. Goldstein, S. A.; Matthews, L. S.; Kuhn, J. L.; Hollister, S. J. *J. Biomech.* **1991**, *24*(Suppl 1), 135–150.
20. Heck, D. A.; Nakajima, I.; Kelly, P. J.; Chao, E. Y. *J. Bone Joint Surg.* **1986**, *68A*, 118–126.
21. Lanyon, L. E.; Paul, I. L.; Rubin, C. T.; *et al. J. Bone Joint Surg.* **1981**, *63A*, 989–1001.
22. Andreykiv, A.; van Keulen, F.; Prendergast, P. J. *J. Biomech. Eng.* **2008**, *130*, 051015-1-11.
23. Engh, C. A.; Bobyn, J. D. *Clin. Orthop.* **1988**, *231*, 7–28.
24. Keaveny, T. M.; Bartel, D. L. *J. Biomech.* **1993**, *26*, 1355–1368.
25. Ko, C. C.; Kohn, D. H.; Hollister, S. J. *J. Mater. Sci. Mater. Med.* **1995**, *7*, 109–117.
26. Rohlmann, A.; Cheal, E. J.; Hayes, W. C.; Bergmann, G. *J. Biomech.* **1988**, *21*, 605–611.
27. Sumner, D. R.; Turner, T. M.; Urban, R. M.; Galante, J. O. *Clin. Orthop. Relat. Res.* **1992**, *276*, 83–90.
28. Bobyn, J. D.; McKenzie, K.; Karabasz, D.; Krygier, J. J.; Tanzer, M. *J. Bone Joint Surg.* **2009**, *91A*, 23–31.
29. Ducheyne, P.; Hench, L. L.; Kagan, A., II; Martens, M.; Bursens, A.; Mulier, J. C. *J. Biomed. Mater. Res.* **1980**, *14*, 225–237.
30. Jasty, M.; Bragdon, C.; Burke, D.; O'Connor, D.; Lowenstein, J.; Harris, W. H. *J. Bone Joint Surg. Am.* **1997**, *79*, 707–714.
31. Mikulec, L. J.; Puleo, D. A. *J. Biomed. Mater. Res.* **1996**, *32*, 203–208.
32. Pilliar, R. M.; Lee, J. M.; Maniatopoulos, C. *Clin. Orthop.* **1986**, *208*, 108–113.
33. Thomas, C. H.; Collier, J. H.; Sfeir, C. S.; Healy, K. E. *Proc. Natl. Acad. Sci.* **2002**, *99*, 1972–1977.

34. van den Dolder, J.; Bancroft, G. N.; Sikavitsas, V. I.; Spauwen, P. H.; Mikos, A. G.; Jansen, J. A. *Tissue Eng.* **2003**, *9*, 505–515.
35. Bobyn, J. D.; Pilliar, R. M.; Binnington, A. G.; Szivek, J. A. *J. Orthop. Res.* **1987**, *5*, 393–408.
36. Crowninshield, R. D.; Brand, R. A.; Johnston, R. C.; Milroy, J. C. *J. Bone Joint Surg.* **1980**, *62A*, 68–78.
37. Willie, B. M.; Yang, X.; Kelly, N. H.; *et al*. *J. Biomed. Mater. Res. B Appl. Biomater.* **2010**, *92*, 479–488.
38. Galante, J. O.; Lemons, J.; Spector, M.; Wilson, P. D., Jr.; Wright, T. M. *J. Orthop. Res.* **1991**, *9*, 760–775.
39. Jacobs, J. J.; Gilbert, J. L.; Urban, R. M. *J. Bone Joint Surg.* **1998**, *80A*, 268–282.
40. Ducheyne, P. *Ann. N. Y. Acad. Sci.* **1988**, *523*, 1–296.
41. Hench, L. L.; Splinter, R. J.; Allen, W. C.; Greenlee, T. K., Jr. *J. Biomed. Mater. Res. Symp.* **1972**, *2*, 117–141.
42. Lord, G.; Bancel, P. *Clin. Orthop.* **1983**, *176*, 67–76.
43. Spector, M.; Davis, R. J.; Lunceford, E. M.; Harmon, S. L. *Clin. Orthop.* **1983**, *176*, 34–41.
44. Pilliar, R. M.; Cameron, H. U.; Macnab, I. *Biomed. Eng.* **1975**, *10*, 126–131.
45. Cook, S. D.; Walsh, K. A.; Haddad, R. J., Jr. *Clin. Orthop.* **1985**, *193*, 271–280.
46. Huiskes, R. In *Functional Behavior of Orthopaedic Biomaterials*; Ducheyne, P., Hastings, G. W., Eds.; Applications; CRC Press: Boca Raton, FL, 1984; Vol. II, pp 121–162.
47. Homsy, C. A.; Cain, T. E.; Kessler, F. B.; Anderson, M. S.; King, J. W. *Clin. Orthop.* **1972**, *89*, 220–235.
48. Tullos, H. S.; McCaskill, B. L.; Dickey, R.; Davidson, J. *J. Bone Joint Surg.* **1984**, *66A*, 888–898.
49. DeMane, M.; Beals, N. B.; McDowell, D. L.; Georgette, F. S.; Spector, M. In *ASTM STP 953 Quantitative Characterization and Performance of Porous Implants for Hard Tissue Applications*; Lemons, J. E., Ed.; ASTM: West Conshohocken, PA, 1987; pp 315–329.
50. Klawitter, J. J.; Bagwell, J. G.; Weinstein, A. M.; Sauer, B. W.; Pruitt, J. R. *J. Biomed. Mater. Res.* **1976**, *10*, 311–323.
51. Rijke, A. M.; Rieger, M. R. *J. Biomed. Mater. Res.* **1977**, *11*, 373–394.
52. Klawitter, J. J.; Hulbert, S. F. *J. Biomed. Mater. Res. Symp.* **1971**, *2*, 161–229.
53. Briggs, E. P.; Walpole, A. R.; Wilshaw, P. R.; Karlsson, M.; Pålsgård, E. *J. Mater. Sci. Mater. Med.* **2004**, *15*, 1021–1029.
54. Walpole, A. R.; Xia, Z.; Wilson, C. W.; Triffitt, J. T.; Wilshaw, P. R. *J. Biomed. Mater. Res. A* **2009**, *90*, 46–54.
55. Ducheyne, P.; Martens, M.; Aernoudt, E.; Mulier, J.; De Meester, P. *Acta Orthop. Belg.* **1974**, *40*, 799–805.
56. Bobyn, J. D.; Stackpool, G. J.; Hacking, S. A.; Tanzer, M.; Krygier, J. J. *J. Bone Joint Surg. Br.* **1999**, *81*, 907–914.
57. Levine, B. *Adv. Eng. Mater.* **2008**, *10*, 788–792.
58. Hahn, H.; Palich, W. *J. Biomed. Mater. Res.* **1970**, *4*, 571–577.
59. Kilner, T.; Pilliar, R. M.; Weatherly, G. C.; Allibert, C. *J. Biomed. Mater. Res.* **1982**, *16*, 63–79.
60. Pilliar, R. M.; Weatherly, G. C. *CRC Crit. Rev. Biocompat.* **1986**, *1*, 371–403.
61. Merget, M.; Aldinger, F. In *Titanium, Science and Technology*; Lutjering, G., Zwicker, U., Bunk, W., Eds.; Deutsche Gesellschaft Fur Metallkunde: Oberursel, West Germany, 1985; pp 1393–1398.
62. Zardiackas, L. D.; Freese, H. L.; Kraay, M. J. *ASTM STP 1471, Titanium, Niobium, Zirconium, and Tantalum for Medical and Surgical Applications*; ASTM: West Conshohocken, PA, 2006.
63. Ducheyne, P.; Kohn, D.; Smith, T. S. *Biomaterials* **1987**, *8*, 223–227.
64. Eylon, D.; Froes, F. H.; Levin, L. In *Titanium, Science and Technology*; Lutjering, G., Zwicker, U., Bunk, W., Eds.; Deutsche Gesellschaft Fur Metallkunde: Oberursel, West Germany, 1985; pp 179–186.
65. Kerr, W. R.; Smith, P. R.; Rosenblum, M. E.; Gurney, F. J.; Mahajan, Y. R.; Bidwell, L. R. In *Titanium '80 Science and Technology*; Kimura, H., Izumi, O., Eds.; The Metallurgical Society of AIME: Warrendale, PA, 1980; pp 2477–2486.
66. Kohn, D. H.; Ducheyne, P. *J. Mater. Sci.* **1991**, *26*, 534–544.
67. Kohn, D. H.; Ducheyne, P. *J. Mater. Sci.* **1991**, *26*, 328–334.
68. Levin, L.; Vogt, R. G.; Eylon, D.; Froes, F. H. In *Titanium, Science and Technology*; Lutjering, G., Zwicker, U., Bunk, W., Eds.; Deutsche Gesellschaft Fur Metallkunde: Oberursel, West Germany, 1985; pp 2107–2114.
69. Ducheyne, P.; Martens, M. *Clin. Mater.* **1986**, *1*, 91–98.
70. Hofmann, A. A.; Bachus, K. N.; Bloebaum, R. D. *J. Arthroplasty* **1993**, *8*, 157–166.
71. Shimko, D. A.; Shimko, V. F.; Sander, E. A.; Dickson, K. F.; Nauman, E. A. *J. Biomed. Mater. Res. B Appl. Biomater.* **2005**, *73*, 315–324.
72. Zardiackas, L. D.; Parsell, D. E.; Dillon, L. D.; Mitchell, D. W.; Nunnery, L. A.; Poggie, R. *J. Biomed. Mater. Res.* **2001**, *58*, 180–187.
73. Levine, B. R.; Sporer, S.; Poggie, R. A.; Della Valle, C. J.; Jacobs, J. J. *Biomaterials* **2006**, *27*, 4671–4681.
74. Patil, N.; Lee, K.; Goodman, S. B. *J. Biomed. Mater. Res. B Appl. Biomater* **2009**, *89*, 242–251.
75. Ducheyne, P.; Van Raemdonck, W.; Heughebaert, J. C.; Heughebaert, M. *Biomaterials* **1986**, *7*, 97–103.
76. Ducheyne, P.; Radin, S.; Heughebaert, M.; Heughebaert, J. C. *Biomaterials* **1990**, *11*, 244–254.
77. Koch, B.; Wolke, J. G. C.; de Groot, K. *J. Biomed. Mater. Res.* **1990**, *24*, 655–667.
78. Segvich, S. J.; Luong, L. N.; Kohn, D. H. In *Biomaterials and Biomedical Engineering*; Ahmed, W., Ali, N., Öchsner, A., Eds.; Trans Tech Publications: Zurich, 2008.
79. Ioku, K.; Yoshimura, M.; Somiya, S. *Biomaterials* **1990**, *11*, 57–61.
80. Kitsugi, T.; Yamamuro, T.; Nakamura, T.; *et al*. *J. Biomed. Mater. Res.* **1986**, *20*, 1295–1307.
81. Knowles, J. C.; Bonfield, W. *J. Biomed. Mater. Res.* **1993**, *27*, 1591–1598.
82. Li, J.; Fartash, B.; Hermansson, L. *Biomaterials* **1995**, *16*, 417–422.
83. Chae, J. C.; Collier, J. P.; Mayor, M. B.; Surprenant, V. A.; Dauphinais, L. A. *J. Biomed. Mater. Res.* **1992**, *26*, 93–102.
84. Koeneman, J.; Lemons, J.; Ducheyne, P.; *et al*. *J. Appl. Biomat.* **1990**, *1*, 79–90.
85. de Groot, K. *Bioceramics of Calcium Phosphate*; CRC Press: Boca Raton, FL, 1983.
86. de Groot, K.; Geesink, R. G. T.; Klein, C. P. A. T.; Serekian, P. *J. Biomed. Mater. Res.* **1987**, *21*, 1375–1381.
87. Ong, J. L.; Harris, L. A.; Lucas, L. C.; Lacefield, W. R.; Rigney, E. D. *J. Am. Ceram. Soc.* **1991**, *74*, 2301–2304.
88. Wolke, J. G. C.; van Dijk, K.; Schaeken, H. G.; de Groot, K.; Jansen, J. A. *J. Biomed. Mater. Res.* **1994**, *28*, 1477–1484.
89. Chai, C. S.; Gross, K. A.; Ben-Nissan, B. *Biomaterials* **1998**, *19*, 2291–2296.
90. Garcia, F.; Arias, J. L.; Mayor, B.; *et al*. *J. Biomed. Mater. Res. (Appl. Biomat.)* **1998**, *43*, 69–76.
91. Gao, Y. In *Biomedical Materials – Drug Delivery, Implants and Tissue Engineering*; Neenan, T., Marcolongo, M., Valentini, R. F., Eds.; Materials Research Society: Warrendale, PA, 1999; pp 361–366.
92. Abe, Y.; Kokubo, T.; Yamamuro, T. *J. Mater. Sci. Mater. Med.* **1990**, *1*, 233–238.
93. Bunker, B. C.; Rieke, P. C.; Tarasevich, B. J.; *et al*. *Science* **1994**, *264*, 48–55.
94. Kohn, D. H. In *Biomedical Engineering and Design Handbook*, 2nd ed.; Kutz, M., Ed.; McGraw-Hill: New York, 2009; Vol. 1, pp 357–381.
95. Tanahashi, M.; Yao, T.; Kokubo, T.; *et al*. *J. Biomed. Mater. Res.* **1995**, *29*, 349–357.
96. Campbell, A. A.; Fryxell, G. E.; Linehan, J. C.; Graff, G. L. *J. Biomed. Mater. Res.* **1996**, *32*, 111–118.
97. Shin, K.; Jayasuriya, A. C.; Kohn, D. H. *J. Biomed. Mater. Res.* **2007**, *83A*, 1076–1086.
98. Wen, H. B.; de Wijn, J. R.; Cui, F. Z.; de Groot, K. *J. Biomed. Mater. Res.* **1997**, *35*, 93–99.
99. Wu, W.; Zhuang, H.; Nancollas, G. H. *J. Biomed. Mater. Res.* **1997**, *35*, 93–99.
100. Combes, C.; Rey, C. *Biomaterials* **2002**, *23*, 2817–2823.
101. Ducheyne, P. *J. Biomed. Mater. Res. Appl. Biomat.* **1987**, *21*(A2), 219–236.
102. Kokubo, T.; Takadama, H. *Biomaterials* **2006**, *27*, 2907–2915.
103. Nakamura, T.; Yamamuro, T.; Higashi, S.; Kokubo, T.; Ito, S. *J. Biomed. Mater. Res.* **1985**, *19*, 685–698.
104. Hanawa, T.; Kon, M.; Ukai, H.; Murakami, K.; Miyamoto, Y.; Asaoka, K. *J. Biomed. Mater. Res.* **1998**, *41*, 227–236.
105. Yamamoto, M.; Kato, K.; Ikada, Y. *J. Biomed. Mater. Res.* **1997**, *37*, 29–36.
106. Kohn, D. H. *Curr. Opin. Solid State Mater. Sci.* **1998**, *3*, 309–316.
107. Du, C.; Cui, F. Z.; Zhu, X. D.; de Groot, K. *J. Biomed. Mater. Res.* **1999**, *44*, 407–415.
108. Hong, S. I.; Lee, K. H.; Outslay, M. E.; Kohn, D. H. *J. Mater. Res.* **2008**, *23*, 478–485.
109. Leonova, E. V.; Pennington, K. E.; Krebsbach, P. H.; Kohn, D. H. *J. Biomed. Mater. Res. A* **2006**, *79A*, 263–270.
110. Kohn, D. H.; Shin, K.; Hong, S. I.; *et al*. In *Proceedings of the 8th International Conference on the Chemistry and Biology of Mineralized Tissues*; Landis, W. J., Sodek, J., Eds.; University of Toronto Press: Toronto, 2005; pp 216–219.
111. Luong, L. N.; Hong, S. I.; Patel, R. J.; Outslay, M. E.; Kohn, D. H. *Biomaterials* **2006**, *27*, 1175–1186.
112. Luong, L. N.; McFalls, K. M.; Kohn, D. H. *Biomaterials* **2009**, *30*, 6996–7004.
113. Segvich, S. J.; Smith, H. C.; Luong, L. N.; Kohn, D. H. *J. Biomed. Mater. Res. B* **2008**, *84B*, 340–349.

114. Kohn, D. H.; Ducheyne, P. In *Medical and Dental Materials*; Williams, D. F., Ed.; VCH: Verlagsgesellschaft, FRG, 1992; pp 29–109.
115. Ducheyne, P.; El-Ghannam, A.; Shapiro, I. *J. Cell. Biochem.* **1994**, *56*, 162–167.
116. El-Ghannam, A.; Ducheyne, P.; Shapiro, I. M. *J. Biomed. Mater. Res.* **1997**, *36*, 167–180.
117. Hartman, E. H. M.; Vehof, J. W. M.; Spauwen, P. H. M.; Jansen, J. A. *Biomaterials* **2005**, *26*, 1829–1835.
118. Krebsbach, P. H.; Kuznetsov, S. A.; Bianco, P.; Gehron-Robey, P. *Crit. Rev. Oral Biol. Med.* **1999**, *10*, 165–181.
119. Ohgushi, H.; Okumura, M.; Tamai, S.; Shors, E. C.; Caplan, A. I. *J. Biomed. Mater. Res.* **1990**, *24*, 1563–1570.
120. Cook, S. D.; Thomas, K. A. *J. Bone Joint Surg. Br.* **1991**, *73*, 20–24.
121. Jasty, M.; Bragdon, C.; Jiranek, W.; Chandler, H.; Maloney, W.; Harris, W. H. *Clin. Orthop. Relat. Res.* **1994**, *308*, 111–126.
122. Kohn, D. H.; Ducheyne, P.; Cuckler, J. M.; Chu, A.; Radin, S. *Med. Prog. Technol.* **1994**, *20*, 169–177.
123. Frost, N. E.; Marsh, K. J.; Pook, L. P. *Metal Fatigue*; Clarendon Press: Oxford, 1974.
124. Cook, S. D.; Georgette, F. S.; Skinner, H. B.; Haddad, R. J., Jr. *J. Biomed. Mater. Res.* **1984**, *18*, 497–512.
125. Georgette, F. S.; Davidson, J. A. *J. Biomed. Mater. Res.* **1986**, *20*, 1229–1248.
126. Margolin, H.; Williams, J. C.; Chesnutt, J. C.; Lutjering, G. In *Titanium '80 Science and Technology*; Kimura, H., Izumi, O., Eds.; The Metallurgical Society of AIME: Warrendale, PA, 1980; pp 169–216.
127. Peters, M.; Gysler, A.; Lutjering, G. In *Titanium '80 Science and Technology*; Kimura, H., Izumi, O., Eds.; The Metallurgical Society of AIME: Warrendale, PA, 1980; pp 1777–1786.
128. Stubbington, C. A.; Bowen, A. W. *J. Mater. Sci.* **1974**, *9*, 941–947.
129. Soltesz, S. M.; Smickley, R. J.; Dardi, L. E. In *Titanium, Science and Technology*; Lutjering, G., Zwicker, U., Bunk, W., Eds.; Deutsche Gesellschaft Fur Metallkunde: Oberursel, West Germany, 1985; pp 187–194.
130. Wolfarth, D.; Filiaggi, M.; Ducheyne, P. *J. Appl. Biomat.* **1990**, *1*, 3–12.
131. Lutjering, G.; Gysler, A. In *Titanium, Science and Technology*; Lutjering, G., Zwicker, U., Bunk, W., Eds.; Deutsche Gesellschaft Fur Metallkunde: Oberursel, West Germany, 1985; pp 2065–2083.
132. Devine, T. M.; Wulff, J. *J. Biomed. Mater. Res.* **1975**, *9*, 151–167.
133. Williams, D. F. In *Biocompatibility of Clinical Implant Materials*, Williams, D. F., Ed.; CRC Press: Boca Raton, FL, 1981; Vol. I, pp 9–44.
134. Placko, H. E.; Brown, S. A.; Payer, J. H. *J. Biomed. Mater. Res.* **1998**, *39*, 292–299.
135. Gilbert, J. L.; Buckley, C. A.; Jacobs, J. J. *J. Biomed. Mater. Res.* **1993**, *27*, 1533–1544.
136. Jacobs, J. J.; Urban, R. M.; Gilbert, J. L.; *et al. Clin. Orthop.* **1995**, *319*, 94–105.
137. Urban, R. M.; Jacobs, J. J.; Gilbert, J. L.; Galante, J. O. *J. Bone Joint Surg.* **1994**, *76A*, 1345–1359.
138. Bartolozzi, A.; Black, J. *Biomaterials* **1985**, *6*, 2–8.
139. Brien, W. W.; Salvati, E. A.; Betts, F.; *et al. Clin. Orthop.* **1992**, *276*, 66–74.
140. Jacobs, J. J.; Skipor, A. K.; Black, J.; Urban, R. M.; Galante, J. O. *J. Bone Joint Surg.* **1991**, *73A*, 1475–1486.
141. Sunderman, F. W., Jr.; Hopfer, S. M.; Swift, T.; *et al. J. Orthop. Res.* **1989**, *7*, 307–315.
142. Agins, H. J.; Alcock, N. W.; Bansai, M.; *et al. J. Bone Joint Surg.* **1988**, *70A*, 347–356.
143. Black, J.; Oppenheimer, P.; Morris, D. M.; Peduto, A. M.; Clark, C. C. *J. Biomed. Mater. Res.* **1987**, *21*, 1213–1230.
144. Brown, S. A.; Farnsworth, L. J.; Merritt, K.; Crowe, T. D. *J. Biomed. Mater. Res.* **1988**, *22*, 321–338.
145. Ducheyne, P.; Healy, K. E. *J. Biomed. Mater. Res.* **1988**, *22*, 1137–1163.
146. Cowin, S. C., Ed.; *Bone Mechanics Handbook*; CRC Press: Boca Raton, FL, 2001.
147. Underwood, E. E. *Quantitative Stereology*; Addison-Wesley: Reading, MA, 1970.
148. Engler, A. J.; Sen, S.; Sweeney, H. L.; Discher, D. E. *Cell* **2006**, *126*, 677–689.
149. Huiskes, R.; Hollister, S. J. *J. Biomech. Eng.* **1993**, *115*, 520–527.
150. Ko, C. C.; Kohn, D. H.; Hollister, S. J. *J. Oral Implantol.* **1992**, *18*, 220–230.
151. Gibson, L. J.; Ashby, M. S. *Proc. R. Soc. Lond.* **1982**, *A382*, 43–59.
152. Simmons, C. A.; Meguid, S. A.; Pilliar, R. M. *J. Orthop. Res.* **2001**, *19*, 187–194.
153. Crowninshield, R. D.; Maloney, W. J.; Wentz, D. H.; Levine, D. L. *Clin. Orthop. Relat. Res.* **2004**, *420*, 176–180.
154. Keaveny, T. M.; Bartel, D. L. *J. Biomech.* **1994**, *27*, 1147–1157.
155. Ramamurti, B. S.; Orr, T. E.; Bragdon, C. R.; Lowenstein, J. D.; Jasty, M.; Harris, W. H. *J. Biomed. Mater. Res.* **1997**, *36*, 274–280.
156. Peterson, C. D.; Hillberry, B. M.; Heck, D. A. *J. Biomed. Mater. Res.* **1988**, *22*, 887–903.
157. Kohn, D. H. *Crit. Rev. Biomed. Eng.* **1995**, *22*, 221–306.
158. Yaszemski, M. J.; Payne, R. G.; Hayes, W. C.; Langer, R. S.; Mikos, A. G. *Biomaterials* **1996**, *17*, 175–185.
159. Li, J. P.; Habibovic, P.; van den Doel, M.; *et al. Biomaterials* **2007**, *28*, 2810–2820.
160. Ishaug-Riley, S. L.; Crane, G. M.; Gurlek, A.; *et al. J. Biomed. Mater. Res.* **1997**, *36*, 1–8.
161. Krebsbach, P. H.; Mankani, M. H.; Satomura, K.; Kuznetsov, S. A.; Gehron-Robey, P. *Transplantation* **1998**, *66*, 1272–1278.
162. Laurencin, C. T.; El-Amin, S. F.; Ibim, S. E.; *et al. J. Biomed. Mater. Res.* **1996**, *30*, 133–138.
163. Gorna, K.; Gogolewski, S. *J. Biomed. Mater. Res.* **2003**, *67A*, 813–827.
164. Li, W. J.; Tuli, R.; Huang, X.; Laquerriere, P.; Tuan, R. S. *Biomaterials* **2005**, *26*, 5158–5166.
165. Nuttelman, C. R.; Tripodi, M. C.; Anseth, K. S. *J. Biomed. Mater. Res.* **2004**, *68A*, 773–782.
166. Payne, R. G.; McGonigle, J. S.; Yaszemski, M. J.; Yasko, A. W.; Mikos, A. G. *Biomaterials* **2002**, *23*, 4381–4387.
167. Marques, A. P.; Cruz, H. R.; Coutinho, O. P.; Reis, R. L. *J. Mater. Sci. Mater. Med.* **2005**, *16*, 833–842.
168. Alsberg, E.; Anderson, K. W.; Alberiuti, A.; Franceschi, R. T.; Mooney, D. J. *J. Dent. Res.* **2001**, *80*, 2025–2029.
169. Kim, H. J.; Kim, U. J.; Vunjak-Novakovic, G.; Min, B. H.; Kaplan, D. L. *Biomaterials* **2005**, *26*, 4442–4452.
170. Holtorf, H. L.; Sheffield, T. L.; Ambrose, C. G.; Jansen, J. A.; Mikos, A. G. *Ann. Biomed. Eng.* **2005**, *33*, 1238–1248.
171. Kruyt, M. C.; Dhert, W. J. A.; Yuan, H.; *et al. J. Orthop. Res.* **2004**, *22*, 544–551.
172. Attawia, M. A.; Devin, J. E.; Laurencin, C. T. *J. Biomed. Mater. Res.* **1995**, *29*, 843–848.
173. Murphy, W. L.; Kohn, D. H.; Mooney, D. J. *J. Biomed. Mater. Res.* **2000**, *50*, 50–58.
174. Thomson, R. C.; Yaszemski, M. J.; Powers, J. M.; Mikos, A. G. *Biomaterials* **1998**, *19*, 1935–1943.
175. Chou, Y. F.; Huang, W.; Dunn, J. C. Y.; Miller, T. A.; Wu, B. M. *Biomaterials* **2005**, *26*, 285–295.
176. Puleo, D. A.; Holleran, L. A.; Doremus, R. H.; Bizios, R. *J. Biomed. Mater. Res.* **1991**, *25*, 711–723.
177. Zreiqat, H.; Evans, P.; Howlett, C. R. *J. Biomed. Mater. Res.* **1999**, *44*, 389–396.
178. James, K.; Levene, H.; Parson, J. R.; Kohn, J. *Biomaterials* **1999**, *20*, 2203–2212.
179. Liu, Y. L.; Hunziker, E. B.; Layrolle, P.; de Bruijn, J. D.; de Groot, K. *Tissue Eng.* **2004**, *10*, 101–108.
180. Shea, L. D.; Smiley, E.; Bonadio, J.; Mooney, D. J. *Nat. Biotechnol.* **1999**, *17*, 551–554.
181. Ripamonti, U.; Ma, S.; Reddi, A. H. *Matrix* **1992**, *12*, 202–212.
182. Sumner, D. R.; Turner, T. M.; Urban, R. M.; *et al. J. Orthop. Res.* **2001**, *19*, 85–94.
183. Midy, V.; Rey, C.; Bres, E.; Dard, M. *J. Biomed. Mater. Res.* **1998**, *41*, 405–411.
184. Ziegler, J.; Mayr-Wohlfart, U.; Kessler, S.; Breitig, D.; Gunther, K. P. *J. Biomed. Mater. Res.* **2002**, *59*, 422–428.
185. Sheridan, M. H.; Shea, L. D.; Peters, M. C.; Mooney, D. J. *J. Control. Release* **2000**, *64*, 91–102.
186. Whang, K.; Tsai, D. C.; Nam, E. K.; *et al. J. Biomed. Mater. Res.* **1998**, *42*, 491–499.
187. Campbell, A. A.; Song, L.; Li, X. S.; *et al. J. Biomed. Mater. Res.* **2000**, *53*, 400–407.
188. Alam, M. I.; Asahina, I.; Ohmamiuda, K.; Takahashi, K.; Yokota, S.; Enomoto, S. *Biomaterials* **2001**, *22*, 1643–1651.
189. Adams, C. S.; Antoci, V., Jr.; Harrison, G.; *et al. J. Orthop. Res.* **2009**, *27*, 701–709.
190. Reiner, T.; Kababya, S.; Gotman, I. *J. Mater. Sci. Mater. Med.* **2008**, *19*, 583–589.
191. Liu, Y. L.; Layrolle, P.; de Bruijn, J.; van Blitterswijk, C.; de Groot, K. *J. Biomed. Mater. Res.* **2002**, *57*, 327.
192. Stigter, M.; de Groot, K.; Layrolle, P. *Biomaterials* **2002**, *23*, 4143–4153.
193. Azevedo, H. S.; Leonor, I. B.; Alves, C. M.; Reis, R. L. *Mater. Sci. Eng. C* **2005**, *25*, 169.
194. Kofron, M. D.; Laurencin, C. T. *Biomaterials* **2004**, *25*, 2637–2643.
195. Li, J. P.; de Wijn, J. R.; van Blitterswijk, C. A.; de Groot, K. *J. Biomed. Mater. Res. A* **2010**, *92*, 33–42.
196. Lin, C. Y.; Wirtz, T.; LaMarca, F.; Hollister, S. J. *J. Biomed. Mater. Res. A* **2007**, *83*, 272–279.
197. Ryan, G. E.; Pandit, A. S.; Apatsidis, D. P. *Biomaterials* **2008**, *27*, 3625–3635.
198. Stevens, M. M.; George, J. H. *Science* **2005**, *310*, 1135–1138.
199. Fujisawa, R.; Mizuno, M.; Nodasaka, Y.; Kuboki, Y. *Matrix Biol.* **1997**, *16*, 21.
200. Segvich, S. J.; Smith, H. C.; Kohn, D. H. *Biomaterials* **2009**, *30*, 1287–1298.